Aquat. Living Resour. 2020, 33, 4
© EDP Sciences 2020
https://doi.org/10.1051/alr/2020005

Aquatic Living Resources
Available online at:
www.alr-journal.org

RESEARCH ARTICLE

Satellite image analysis reveals changes in seagrass beds at Van Phong Bay, Vietnam during the last 30 years

Trong-Thach Vo[1], Khin Lau[2], Lawrence M. Liao[3] and Xuan-Vy Nguyen[2,4,*]

[1] Nha Trang Institute of Technology Research and Application, Viet Nam Academy of Science and Technology, 02 Hung Vuong, Nha Trang City, Viet Nam
[2] Institute of Oceanography, Viet Nam Academy of Science and Technology, 01 Cau Da, Nha Trang City, Viet Nam
[3] Graduate School of Integrated Sciences for Life, Hiroshima University, 1-4-4 Kagamiyama, Higashi-Hiroshima City, Hiroshima 739-8528, Japan
[4] Graduate University of Science and Technology. 18 Hoang Quoc Viet, Cau Giay, Ha Noi, Viet Nam

Received 4 November 2019 / Accepted 22 March 2020

Handling Editor: David Kaplan

Abstract – Seagrass meadows are fragile ecosystems in the coastal zone. Natural disasters, land reclamation and various human activities seem to exert negative impacts on the distribution and biological performance of seagrass beds in Vietnam. In this present study, satellite Landsat TM/OLI image analysis was applied to determine changes in seagrass distribution at Van Phong Bay, Vietnam in the last 30 years. The maximum likelihood decision rule was used to extract seagrass bed distribution data. The error matrix using the in situ reference data for HLM image classification was 81–95% accurate, and Kappa coefficients were between 0.72 and 0.91. The results indicated that 186.2 ha (or 35.8%) of the original seagrass beds were lost in the last three decades at Van Phong Bay, and decline in each specific site may have been due to different causes. Typhoons may have caused the loss of seagrass beds at open-sea sites whereas aquaculture activities, excavation and terrigenous obliteration may have caused such losses in protected sites.

Keywords: aquaculture / remote sensing / seagrasses / typhoons

1 Introduction

Seagrasses are fully submerged marine angiosperms and widely distributed throughout the tropical and temperate regions. Like mangroves, they are important coastal ecosystem engineers that can act upon the physical environment mainly by controlling erosion through their well-developed root systems (Uhrin and Turner, 2018). In addition, seagrass beds can reduce the physical impact of waves and current energy as water passes through the densely packed intertidal meadows. They also act as biological filters by trapping fine sand and particulates that may otherwise be suspended in the water column, and thereby contributing to greater water clarity (Lemmens et al., 1996). In addition, the multiple roles of seagrasses are reflected in many biological, physical and chemical aspects (Scott et al., 2018). It is also well known that many marine species utilize seagrass habitats as feeding grounds and nursery areas (McCloskey and Unsworth, 2015). Many species spend their juvenile stage in seagrass beds, eventually moving on to mangroves as they mature (Jaxion-Harm et al., 2012; Honda et al., 2013).

However, seagrass meadows are fragile coastal ecosystems. Since 1980, a global assessment showed that the area of seagrass beds worldwide is decreasing at a rate of 110 km^2 yr^{-1} (Waycott et al., 2009). In Cockburn Sound (Western Australia), another study reported that 75% of seagrasses (2169 ha) were lost in the 1960s–1980s due to poor water quality (Fraser and Kendrick, 2017). Human-induced disturbances, pathogens, weather extremes, and climate change are among the causes of significant losses in seagrass beds (Duarte et al., 2008). For example, effluents of pond aquaculture exerted negative impacts on the distribution and performance of seagrasses in Hainan, China (Herbeck et al., 2014). Fishing and industrial activities have disturbed seagrass meadows worldwide (Nadiarti et al., 2012; Nordlund et al., 2018). Yang and Yang (2014) indicated that the seagrass beds have been also greatly affected by typhoons, even those in subtidal depths of up to 27 m (Colin, 2018). Typhoons are growing in intensity and frequency thus increasing water turbulence that inflict direct physical damage.

Due to degradation of seagrass at the global scale, several monitoring programs were developed for the detection of changes in cover, biomass, and density in different regions and in countries such as USA (Neckles et al., 2012), Australia

*Corresponding author: nguyenxuanvi@gmail.com

(McKenna et al., 2015), the Mediterranean region (Royo et al., 2010), as well as in neighboring countries of Vietnam including Thailand (Rattanachot et al., 2018), Indonesia (Nadiarti et al., 2012), and the Philippines (Fortes, 2012). Several methods have been applied to monitor the seagrass meadows in recent years. These include single-beam sonar (Sabol et al., 2002), multiscan sonar (Montefalcone et al., 2006), surface-based videography (Neckles et al., 2005), direct observation (Short et al., 2006), underwater videography (Schultz, 2008), lightweight drone (Duffy et al., 2018) and remote sensing (RS) via satellite or airplane (Hossain et al., 2015). Among them, remotely sensed imagery has been the most widely used method for mapping numerous habitats, including seagrass (Yang and Yang, 2009). Therefore, the increasing use of RS methods became an essential supplement to the conventional method because of their efficiency, large area of coverage, and repeatability of observations (Hossain et al., 2015).

In Southeast Asia, the seagrass distribution is nearly 37,000 km^2 but this is likely an underestimate as some countries in the region are not well studied and detailed information is lacking (Fortes et al., 2018). In the same way, studies on seagrass distribution in Vietnam are still lacking. The coast of Khanh Hoa province consists of bays and lagoons where seagrass meadows occupy an area of about 1,682 ha (Nguyen et al., 2017a). There are three main seagrass beds here including Van Phong Bay (VPB), Thuy Trieu lagoon and Cam Ranh Bay. Additionally, a high human population (approximately 1,230,000) exists there and many industries including seafood processing companies, shipyards and sugar refinery plants are fast developing along the coast. Industrialization and rapid urbanization along coastal areas have increased since the 2000s. Hence, anthropogenic impacts may pose great threats causing seagrass degradation in this area (Nguyen et al., 2017b). By using TM/ETM+/OLI imageries, Chen et al. (2016) found that the total area of seagrass beds at Cam Ranh Bay had declined by approximately 25% (66 ha), which they attributed to coastal development and infrastructure construction from 1996 to 2015. On the other hand, monitoring and detection of changes of seagrass beds in VPB have been very limited although this seagrass habitat is considered as one of the biggest in Vietnam. The present study seeks to investigate the current coverage, species composition, biomass and shoot density, and document coverage changes of seagrass beds in VPB from 1988 to 2019 using satellite image analysis, especially considering the devastating impacts of strong typhoons on seagrass distribution at VPB during the last three decades.

2 Materials and methods

2.1 Study areas

VPB is located in the northern section of Khanh Hoa province, Vietnam, between 12.79° – 12.47°N and 109.20° – 109.44°E (Fig. 1). The coastline is approximately 100 km long. The discontinuous seagrass beds were found mainly at three locations namely My Giang (MG), Tuan Le (TL) and Xuan Tu (XT). Among seagrass beds at VPB, MG has shown the highest species diversity with six species while only four and two were found at TL and XT, respectively

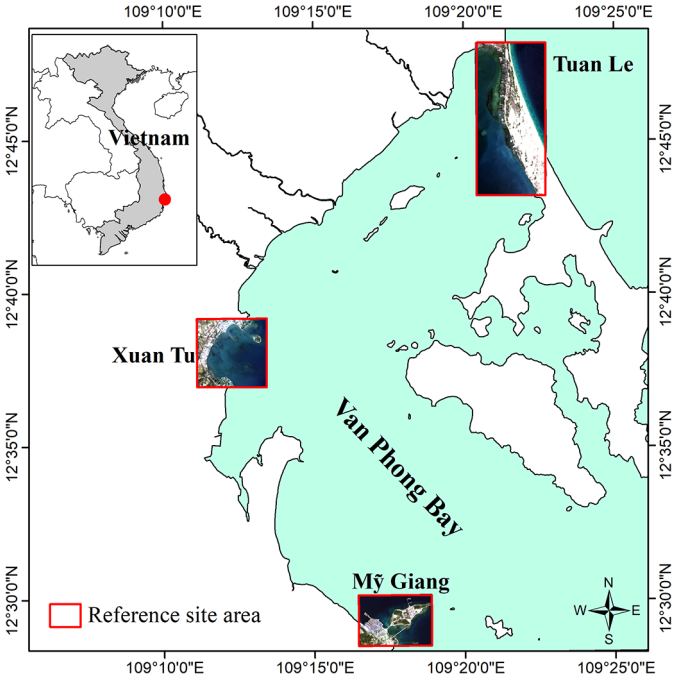

Fig. 1. Map of Van Phong Bay (VPB) and the three main seagrass beds at Tuan Le (TL), Xuan Tu (XT) and My Giang (MG). The frames represented positions of acquired satellite images. The map was processed by MapInfor Pro™, version 12.5.5 (Pitney Bowes Software Inc., NY, USA).

(Nguyen et al., 2010). Shipyard industries are concentrated near MG seagrass beds whereas shrimp ponds and marine culture cages are plentiful at TL and XT, respectively (Statistics Office of Khanh Hoa Province, 2010 and 2018). The substrata are varied among locations with shallow dense and patchy seagrass beds, bare shallow muddy sand, and deeper water without seagrass at TL (Fig. 2). At XT, the different substrata include seagrass beds, muddy sand with rocks and reef/sandy bottoms (Fig. 3). The same bottom types occur in MG and at XT. In general, the salinities at VPB are between 34.8‰ and 35.5‰ in the dry season, and 32‰ in the rainy season. Emersion time of seagrass and Secchi depth also showed high variability between rainy (monsoon) and dry seasons. The longest emersion time and the greatest Secchi depth were 5 h and 6 m in July, respectively, while the shortest emersion time and shallowest Secchi depth were 1 h and 1 m in February, respectively. There were nine tropical storm/typhoons that passed through VBP from 1993 to 2017, five of which were categorized as class TY (typhoon, 64–105 kt) In particular, typhoons Lola (105 kt, December 1993) and Damrey (90 kt, November 2018) were considered as two of the strongest typhoons that ravaged VPB (www.coast.noaa.gov/hurricanes/?redirect=301ocm).

2.2 Data collection

A total of 14 scenes of Landsat cloud-free data (path/row =123/51) from 1988 to 2019 that covered VPB and acquired from the United States Geological Survey (USGS) were used in this study. Among them, 10 scenes were Landsat 5 TM and 4 scenes were Landsat 8 OLI satellite images. Detailed

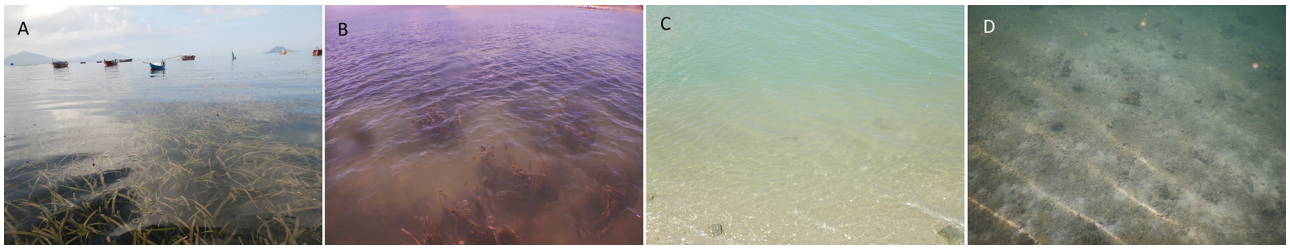

Fig. 2. Different shallow substrata at TL, A = shallow dense seagrass beds, B = shallow patchy seagrass beds, C = shallow muddy sand, and D = deeper water with sand substratum. See Figure 1 for the abbreviation of locations.

Fig. 3. Different shallow substrata at XT, A = seagrass beds, B = muddy sand with rock and C = the reef/sand substratum. See Figure 1 for the abbreviation of locations.

Table 1. Sensor type, acquisition date and time of satellite image data sets used in the present study.

No	Name of satellite scene	Time of acquisition (UTC + 07:00)	Acquisition date
1	Landsat 5 TM	09:31:37	Jun. 8, 1988
2	Landsat 5 TM	09:21:18	Mar. 26, 1990
3	Landsat 5 TM	09:21:02	Apr. 22, 1994
4	Landsat 5 TM	09:12:57	May 26, 1996
5	Landsat 5 TM	09:27:47	Mar. 29, 1997
6	Landsat 5 TM	09:37:41	Mar. 16, 1998
7	Landsat 5 TM	09:36:04	Apr. 22, 2000
8	Landsat 5 TM	09:40:11	Mar. 16, 2004
9	Landsat 5 TM	09:55:09	Mar. 25, 2007
10	Landsat 5 TM	09:50:30	Jun. 8, 2011
11	Landsat 8 OLI	10:01:38	Mar. 12, 2014
12	Landsat 8 OLI	10:01:18	Sep. 28, 2017
13	Landsat 8 OLI	10:00:19	Apr. 24, 2018
14	Landsat 8 OLI	10:00:35	Apr. 11, 2019

information for the satellite image data sets including sensor type, acquisition date and time are presented in Table 1. Landsat TM data have 7 spectral bands, with a spatial resolution of 30 m for bands 1−5 and 7. TM band 6 (thermal infrared) was acquired at 120 m resolution. Landsat 8 OLI data have 8 spectral bands with a spatial resolution of 30 m for bands 1−7 and 9, one panchromatic band with a spatial resolution of 15 m for band 8, and 2 thermal infrared bands with a spatial resolution of 100 m for bands 10 and 11. In this study, 4 spectral bands for Landsat 5 TM and 5 bands for Landsat 8 OLI of data were used for the classification, specifically bands 1–4 in Landsat 5 TM, and bands 1–5 in Landsat 8 OLI. Ground survey for seagrass bed distribution data in TL, XT, and MG were carried out during dry (June 2018 and March 2019) and rainy season (October 2018) by walking during low tide period and using a small fishing boat with the aid of Global Positioning System (GPS, Ashtech Ppromark2 GPS Survey Unit, Thales Navigation, Santa Clara, CA, USA) for position, underwater camera (Nikon CoolPix W300 and Pentax Option WG-2 GPS, Tokyo, Japan), and a sheet note at each site chosen. The ground survey points of seagrass and non-seagrass were chosen based on the pre-identification from review of the satellite imagery and historical research. At each point, ground substratum, seagrass cover and diversity were collected by using quadrat frame, GPS and camera. For each substrate (dense seagrass, patchy seagrass beds, shallow muddy sand, deeper sandy substratum, muddy sand with rocky substratum and reef/sand substratum) more than 50 points were recorded in each region for image interpretation and validation.

For the ancillary historical data used here including seagrass shoot density and biomass, the cover of seagrass and other ground reference were collected in 1996 and have been reported by Pham et al. (2006), while data collected in 2010 and 2014 have been reported by Nguyen et al. (2010) and Nguyen and Nguyen (2014), respectively (Table S1). In this present study, shoot density, biomass, seagrass cover and ground reference data of seagrass were collected at fourteen stations. Sample and data collection were done following the protocol of Short et al. (2006). Seagrass percent cover by species was visually estimated in each quadrat. The total biomass was collected with a 0.25 m^2 quadrat outside each quadrat at least 5 m distance from the quadrat but in an area of

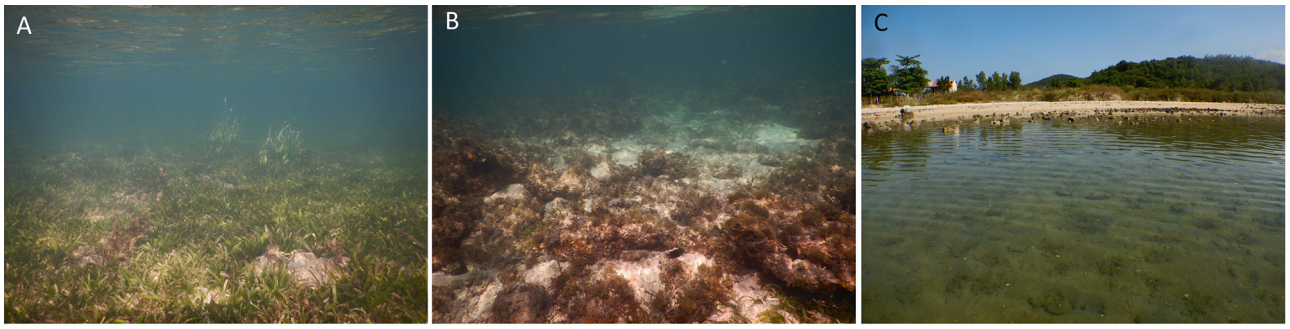

Fig. 4. Different shallow substrata at MG. See Figure 3 for the abbreviation of locations. Sea Figure 3 for the kinds of substratum.

the same seagrass species and cover. Epiphytes were removed from the leaves. All plant parts were rinsed in freshwater, and dried at 60 °C until constant weight was obtained (Short et al., 2006). The field study was carried out in March 2019.

2.3 Data analysis

The seagrass bed maps in TL, XT, and MG were derived from Landsat 5 TM and 8 LOI images. The images in staged time were first cleared of the atmospheric effect by "dark spectrum fitting" atmospheric corrected approach (Vanhellemont and Ruddick, 2018; Vanhellemont, 2019) via ACOLITE processor. Areas that were not of interest, including bare substratum and lands were manually masked out. The sun glint on the images also was removed by using the brightness in a near-infrared (NIR) band following the method of Hedley et al. (2005). The seagrass beds in TL, XT, and MG were previously found to be distributed in very shallow water at less than 2 m (Pham et al., 2006; Nguyen and Nguyen, 2014), where the reflectance is mostly affected by bottom types. The water column correction was ignored (Lyzenga, 1978; Sagawa et al., 2010). Ground truth data was generated by experienced interpreters from each year's imagery using all available field data for 145, 75, and 69 sites at TL, XT, and MG respectively. The ground truth data for each year was divided into two datasets, the first contained around 70% of all data was used for a classification model, and the remaining 30% of the data was used for validation (Table S1). In this present study, we used the maximum likelihood decision rule (MLC) to classify the images. To improve the classification results, the seagrass beds in TL were divided into two classes, patchy and dense seagrass bed. For a pixel on the patchy seagrass beds, the percentage of sand substratum was always higher than the percentage on the dense seagrass beds. This has caused the differences of spectral reflectance values on patchy and dense seagrass beds. The range of the difference values may include other substrata. Therefore, four classes including dense seagrass beds (Figure 2A), patchy seagrass beds (Figure 2B), shallow muddy sand substratum (Figure 2C), and deeper sand substratum (Figure 2D) were used to do classification in this area. The seagrass beds at XT and MG are more homogeneous and cannot be separated into dense or patchy seagrass. Thus, three classes including seagrass bed (Figures 3A and 4A), muddy sand with rocky substratum (Figures 3B and 4B) and reef/sand substratum (Figures 3C and 4C) were used for the classified images. The 'salt-and-pepper' noises in the classified results were removed by using a median filter. We validated the mapping results by using overall accuracy (OA) that indicated the percentage of correctly classified test data on total test data without regard to class memberships and Kappa coefficient (Kappa) to measure the agreement between classified results and test data with the possibility of the agreement occurring by chance on classified memberships (Cohen, 1960). Both OA and Kappa were obtained from confusion matrix (Congalton, 1991). Finally, the non-seagrass classes were removed and the remaining seagrass beds class was used to analyze the changes in the VPB.

3 Results

3.1 Current status of seagrass beds in Van Phong Bay

The total area of seagrass beds at VPB was found to be 334.1 ha in 2019. The largest area recorded at TL was 246.7 ha while those numbers at XT and MG were 59.4 and 28 ha, respectively. The species composition varied among the beds. Six species including *Enhalus acoroides* (Linnaeus *f.*) Royle, *Thalassia hemprichii* (Ehrenberg) Ascherson, *Halophila ovalis* (R. Brown) J.D. Hooker (all belonging to the Hydrocharitaceae), *Halodule uninervis* (Forsskål) Ascherson, *Halodule pinifolia* (Miki) Hartog, *Cymodocea rotundata* Ascherson *et* Schweinfurth and *Cymodocea serrulata* (R. Brown) Ascherson *et* Magnus (all belonging to the Cymodoceaceae) were recorded, and two species: *Enhalus acoroides* and *Thalassia hemprichii* were dominant at the three main beds. *Cymodocea serrulata* was the only species occurring at MG. At TL, *Enhalus acoroides* formed the vast monospecific beds while *Thalassia hemprichii* occurred in patchy beds below *Enhalus acoroides* in some cases. Shoot density of *Enhalus acoroides* was 136 ± 35 shoots.m^{-2} whereas the shoot density of *Thalassia hemprichii* was 420 ± 35 shoots m^{-2}. The cover of *Enhalus acoroides* and *Thalassia hemprichii* were $73.8 \pm 5\%$ and $35.7 \pm 12\%$, respectively.

3.2 Seagrass mapping accuracy

Three spectral reflectance profiles of different substrata at TL, XT and MG indicated that the reflectance values of the dense seagrass beds at the three sites were lower than the

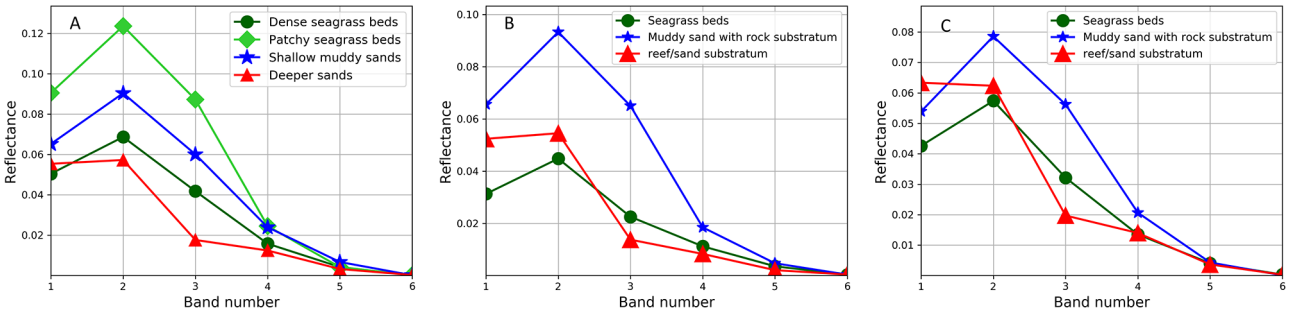

Fig. 5. Spectral reflectance profiles of different substrata at TL, XT and MG in different bands. A = TL, BXT and C = MG. See Figure 1 for the abbreviation of locations.

Table 2. Error matrix of the comparison between the maximum likelihood decision rule (MLC) image classification and ground truth surveys. The numbers in bold indicate the overall accuracy and Kappa coefficient (Kappa). See Fig. 1 for the abbreviation of locations.

		1988	1990	1994	1996	1997	1998	2000	2004	2007	2011	2014	2017	2018	2019
TL	OA (%)	95	86.4	88.2	92	88.6	86.7	86.1	86.9	89.7	86	89.8	87.9	87	85.5
	Kappa	0.92	0.82	0.82	0.89	0.84	0.82	0.81	0.82	0.86	0.8	0.86	0.83	0.83	0.8
XT	OA (%)	92.8	87.8	93.3	91	89.6	87.8	89.9	91	94	88.1	91	87.2	91	87.8
	Kappa	0.89	0.82	0.9	0.86	0.84	0.82	0.85	0.87	0.91	82	0.86	0.8	0.87	0.82
MG	OA (%)	90.9	87.9	92.4	84.9	90.3	85.1	84.9	91.2	88.3	88.3	83.1	85.9	82.2	88.4
	Kappa	0.86	0.81	0.88	0.76	0.85	0.77	0.77	0.85	0.81	0.81	0.73	0.78	0.72	0.81

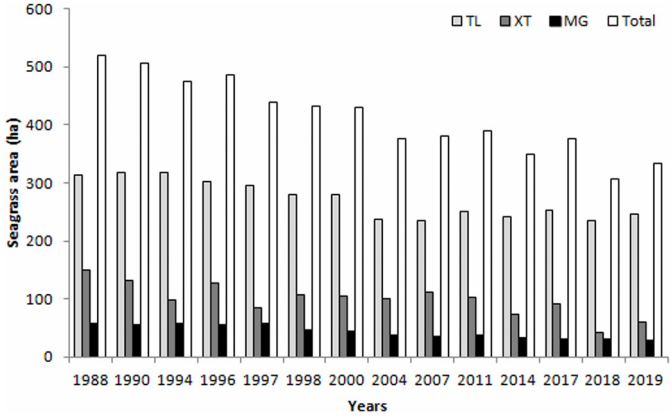

Fig. 6. Change detection of seagrass beds at TL (25% solid background), XT (50% solid background), MG (100% solid background) and the total (blank) 1988 to 2019. See Fig. 1 for the abbreviation of locations.

reflectance values of shallow muddy sand in four bands (band 1 of green (485 nm), band 2 of blue (560 nm), band 3 of red (660 nm) and band 4 of NIR (830 nm)). The patchy seagrass beds in TL showed the highest reflectance values on bands 1, 2 and 3, whereas reflectance values of the reef/sand substratum at XT and MG were highest at band 2 (Fig. 5). Using MLC classifier, the patchy and dense seagrass beds were combined as seagrass beds in green color (Fig. 6). The non-seagrass beds substratum was removed. The classification results were assessed by comparing with the ground reference data (Table S2). The overall accuracies (OA) and Kappa coefficients (Kappa) obtained from confusion matrix were generally higher than 82% and 0.72, respectively (Tab. 2).

3.3 Detected changes in seagrass beds

In general, total seagrass distribution at VPB has continuously decreased since 1988 (Fig. 6). There were 186 ha (or 35.8%) lost between 1998 and 2019. For the first ten years (1988–1998, the first decade), the results indicated that seagrass beds were decreasing at a rate of 8.7 ha year^{-1} equal to 1.68% per year. The beds lost 52.5 ha or 12.1% in the next decade (1998–2007, second decade). Finally, seagrass distribution further declined by 46.5 ha (12.2%) from 2007 to 2019 (third decade). Comparing the three sites, the highest decline of seagrass beds was found at TL where 41.3 ha (or 14.8%) was lost during the period 2000–2004 whereas there were only a few changes before and after that period. Therefore, the decline of seagrass distribution at TL occurred mainly during the second decade. Compared to TL, seagrass beds at XT declined during both the first and third decades, with recovery observed during the second decade. For the first decade, two drops were recorded in 1994 and 1997 at 33.6 and 41.1 ha, respectively (comparing data in 1990 and 1996). In the second decade, seagrass beds at XT increased by 4.6 ha. However, the total seagrass distribution in VPB had lost 51.7 ha, the highest loss recorded in 2018 with nearly 50 ha lost (comparing to the data in 2017). Hence, the seagrass meadows at XT lost a total of 89.6 ha (60.1%) in the last three decades. At MG, a significant decline of seagrass beds occurred

consistently for three decades with 7–12 ha lost in each decade. The current seagrass beds at MG was 28 ha (2019), much lower than 58.7 ha in 1988. Finally, a total of 186 ha (or 35.8%) of seagrass beds was lost in the last three decades throughout the VPB. Among the three sites within VPB, XT showed the highest loss (61.1%), followed by MG (52.3%) and TL (21.1%). The detected changes of seagrass at VPB from 1998 to 2019 are presented in Figure 7.

4 Discussion

Among fragile marine ecosystems, seagrass beds have been seriously impacted and degraded globally. The present study used integrated Landsat 5 TM and 8 OLI imageries for the first time in this region to reveal significant changes of seagrass distribution at the local scale, specifically within the VPB.

The seagrass bed spectral reflectance profile in VPB was found to be similar to the spectral reflectance profiles in Cam Ranh Bay, Vietnam (Chen et al., 2016), Funakoshi Bay, Japan and Mahares, Tunisia (Sagawa et al., 2010) where the near infrared (NIR) band value was smaller than the red, blue and green value bands (Fig. 3). It was, however, different from the studies of Kim et al. (2015) and Barillé et al. (2010), in which the NIR band showed the highest values while other barren underwater substrata showed lower values in the NIR band. This could be explained by using the satellite acquired time and seagrass beds exposure period. The NIR band value would be very low due to the absorption of the water (Lyzenga, 1978). The emersed seagrass beds at the time, like vegetation on land, got a high reflectance in the NIR band which could be using NDVI (Normalized Difference Vegetation Index) to extract the seagrass bed from satellite data. In this study, the Landsat images were not applied for water column correction because the seagrass beds in VPB were located in very shallow water (<2 m depth) and focused on the seagrass beds region only, masking out the non-vegetated areas. It is a little bit different when compared to previous studies (Chen et al., 2016; Sagawa et al., 2010), therefore, the classification result showed that OA and Kappa were higher than 82% and 0.72, respectively.

Decline of seagrass distribution at TL started from 2004. Our findings revealed that the distribution of seagrass meadows had declined by 22.1% with a decreasing annual trend of 12.2 ha. The main causes of seagrass bed loss were related to the conversion of the seagrass meadows into shrimp ponds. There are no available reports on the extent of shrimp ponds developed during that period. However, our satellite image analysis indicated that the shrimp ponds appeared in 2000 on parts of seagrass beds. Recently, Chen et al. (2016) indicated that some seagrass beds have been destroyed or declined due to culture farms constructed directly on the seagrass areas as in the case of Thuy Trieu lagoon, Vietnam. The previous report of Pham et al. (2006) showed that seagrass beds in the coastal waters of Khanh Hoa province were lost or reduced up to 30% of the original areas during the period 1996–2002 due to several factors. Among them, extensive shrimp farming was identified as the main factor. On another hand, pond aquaculture effluents were also considered to be the major determinants of seagrass degradation (Herbeck et al., 2014). Untreated aquaculture effluents cause coastal eutrophication that may be especially harmful to seagrass beds (Herbeck et al., 2013; Govers et al., 2014).

Decline of seagrass distribution at MG occurred from 1998 through 2004. The Hyundai-Vinashin Shipyard Co., Ltd erected its facilities at MG in 1998 (http://www.hyundai-vinashin.com/vn/aboutus/history.php). Excavation and terrigenous obliteration may be the main causes of seagrass bed loss in this area. Our analysis indicated that 28 ha (57%) of seagrass beds were lost at MG during the above period while the satellite image analysis also revealed 12.7 ha of tidal flat including seagrass beds were reclaimed for the construction of various factories. Unfortunately, there was no recovery of seagrass beds at MG after the year 2004. Excavation, transportation, and disposal of soft-bottom material may lead to various adverse impacts on the marine environment that have negative effects on seagrass beds (Bourque et al., 2015). A previous study showed that the total daily deposition measured with sediment traps was about 681 g DW m^{-2} day^{-1} in seagrass beds at MG, much higher than other locations in South East Asia (Gacia et al., 2003). Several studies indicated that excess Cu can cause chlorosis, inhibition of root growth and damage to plasma membrane permeability and may lead to ion leakage in plants (De Vos et al., 1991; Papenbrock, 2012). Some evidences indicated that ships undergoing repair at the shipyard in MG may be the source of Cu (Dung et al., 2014; Nguyen et al., 2017a) that has been linked to the decline of seagrass beds at MG. The results of Bourque et al. (2015) indicated that disturbance involving excavated surface soils resulted in long-term losses of seagrass in Florida. In another case involving *Zostera noltii* in Arcachon Bay (France), seagrasses needed more than five years to recover from dredging activities (Tu et al., 2012). In the Philippines, immediate causes of degradation of seagrass were traced to industrial and port development as well as recreational activities (Kirkman and Kirkman, 2002).

Among surveyed locations at VBP, the seagrass beds at XT may have declined due to both natural causes and human-induced activities. There were three episodes of extreme decline in the years 1994, 1997 and 2017. Marine cage culture of lobsters has increased in XT since 1992 (Le and Nguyen, 2004). The study of Uhrin and Fonseca (2005) indicated that lobster cage culture in Florida resulted to significantly decreased shoot densities of seagrass. Indirectly and potentially so, the impacts of water quality degradation resulting from increased nutrient additions have caused seagrass loss (Waycott et al., 2009). Ruiz et al. (2001) showed that the shoot size, leaf growth rate and the number of leaves per shoot of seagrass close to a fish farm in Spain decreased due to poor water transparency and increasing dissolved nutrient and organic content of sediments in the vicinity of those cages. Our results showed that seagrass beds at XT were markedly lower in 1994 and 2018 after typhoons Lola (wind speed, 105 kt) and Damrey (wind speed, 90 kt) directly hitting VPB in 1993 and 2017, respectively (Tab. 3, Fig. 8). Hurricanes also caused direct and immediate seagrass loss due to the velocity of the current, increasing turbulence and re-suspending sediments (Orth et al., 2006; Yang and Yang, 2014). Hurricanes often cause erosion or deposition of sediments that may uproot or obliterate seagrass beds (Fourqurean and Rutten, 2004). Our study indicated that 32.5 and 46.4% of seagrass distribution disappeared after the occurrence of typhoons Lola and

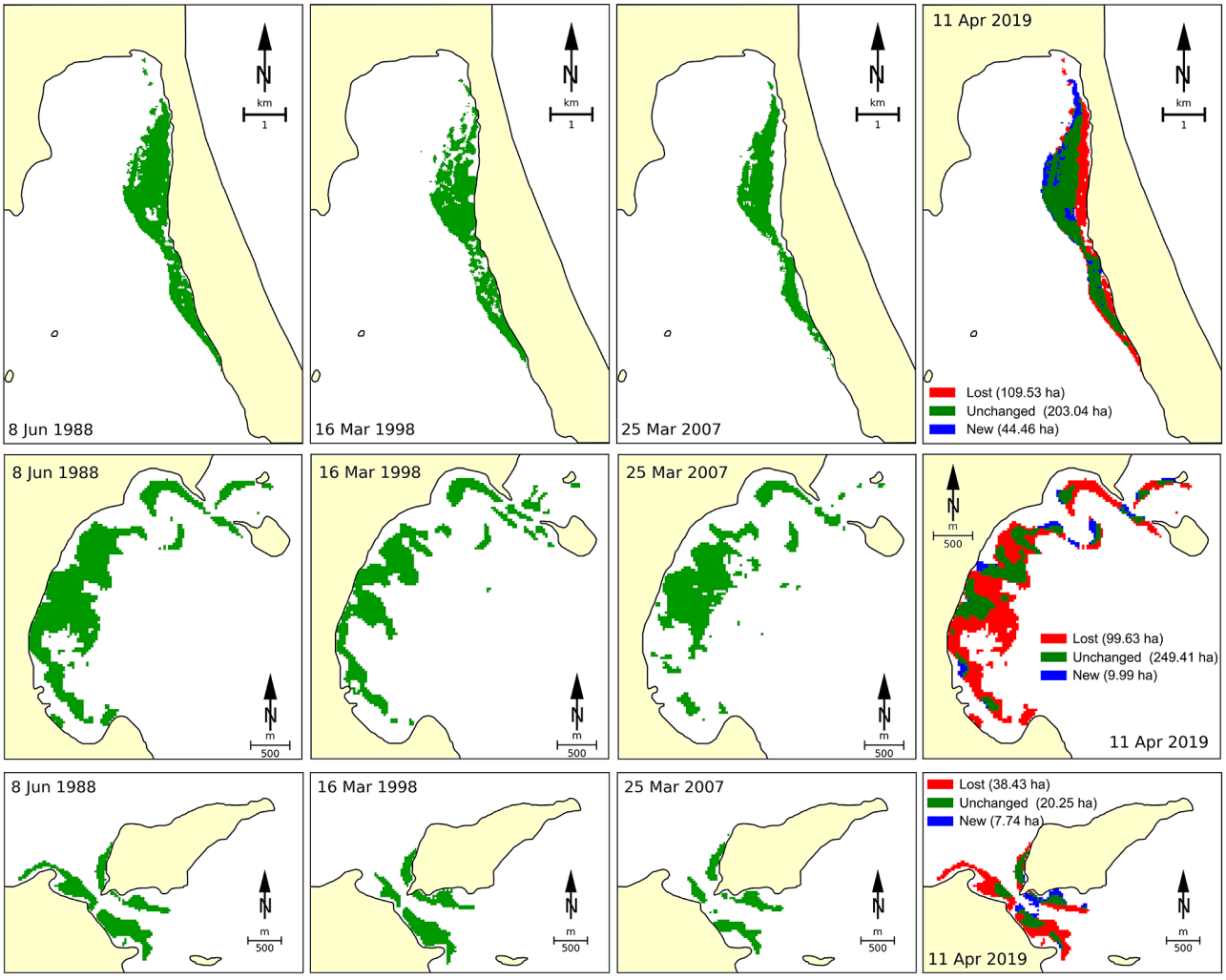

Fig. 7. Change detection of seagrass beds in 1988, 1998, 2007 at 2019 at VPB. Left to right, the first, second and third rows present change detection of seagrass beds at TL, XT and MG respectively. In the satellite image classification, the unchanged seagrass beds are represented as green color in each specific years, the new and lost seagrass beds are represented in blue and red colors. See Figure 1 for the abbreviation of locations.

Table 3. List of typhoons and its characters affecting the Khanh Hoa coast including VPB during 1988 to 2019 (Source: https://coast.noaa.gov/hurricanes/?redirect=301ocm). T = Typhoon. TS = Tropical storm. 1, 2, 3 are the levels of category following those of Saffir-Simpson (USA).

Name of typhoons	Lola	Kyle	Yvette	Faith	Mirinae	Hagupit	Sinlaku	Damrey	Kigori
Category	T3	T2	T1	T2	T2	TS	TS	T2	TS
Date	Dec 1993	Nov 1993	Oct 1995	Dec 1998	Nov 2009	Dec 2014	Nov 2014	Nov 2017	Nov 2017
Max wind speed (kt)	105	95	65	90	90	45	55	90	40

Damrey, respectively. At Jangheung Bay (Korea), field observation and satellite images showed that there was a die-off of seagrass in September 2012 after typhoons Bolaven, Tembin, and Sanba passed through the site one after another (Kim et al., 2015). In the same way, 70% of seagrass in one section of Carpentaria Bay, Australia was destroyed by the cyclone Sandy (Poiner et al., 1989). Another report of Preen et al. (1995) indicated that 24% (approximately 1000 km^2) of seagrass was lost in Hervey Bay, Australia after another cyclone in 1992. However, another study reported that only a little change was detected among the seagrass beds in the Gulf of Mexico after hurricane Katrina hit in August 2005 (Anton et al., 2009). Our results indicated that the seagrass meadows at TL and MG seem to show no detectable changes after two typhoons (Lola and Damrey) hit. The topography of VPB (Fig. 1) shows that seagrass beds at TL and MG seemed to be protected by a peninsula and MG Island, whereas seagrass beds at XT were exposed to the open-sea to the east. The latter

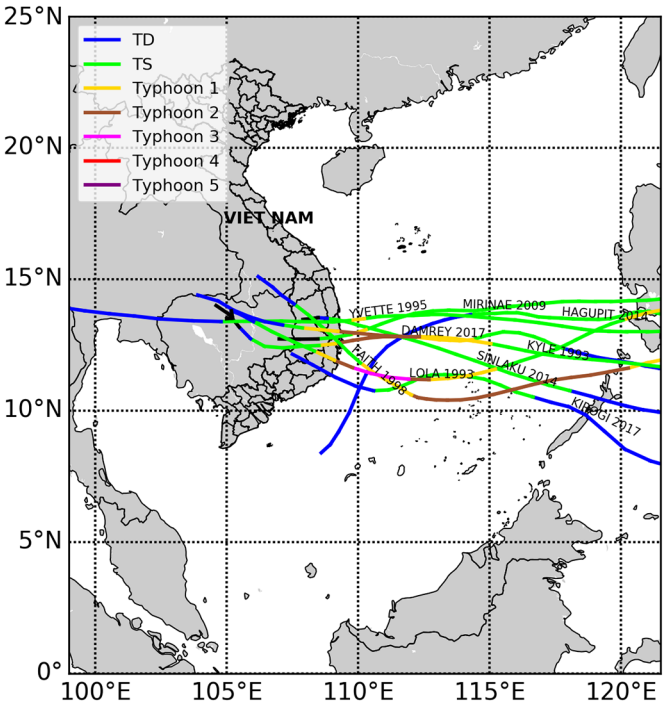

Fig. 8. Pathway of strong typhoons affecting VPB from 1951 to 2017.

may explain the physical decline of seagrass beds at XT after typhoon events. The report of Yang and Huang (2011) also showed that typhoons Tianying and Dawei just slightly impacted two apparently protected sites among three surveyed sites at Hainan, China. Therefore, typhoons did not seem to disturb all seagrass beds within the VPB. Seagrass beds show natural temporal variability but also have resistance against disturbances from typhoons (Steward et al., 2006; Kim et al., 2015). Our analysis revealed that seagrass beds at XT somewhat recovered after destructive climatic events. Only one year after each typhoon (Lola in 1993 and Damrey in 2017), there was slight natural recovery of 12.5 and 7.5 ha (or 13.2 and 15.5%) seagrass beds at XT, respectively. The study of Hiraoka et al. (2016) showed that natural *Zostera* beds in Hiroshima, Japan naturally recovered two years after typhoon attacks, while there was no recovery of the seagrass beds at Jangheung Bay, Korea after such destructive weather episodes (Kim et al., 2015).

5 Conclusion

Information on seagrass distribution in VPB spanning 30 years (1988–2019) was quantified using satellite remote sensing data and ground survey information. The total area of seagrass distribution was 334.1 ha in 2019, accounting for a loss of 186.2 ha or 35.8% compared to the data in 1988. Comparisons among each decadal periods (1988–1998, 1998–2007 and 2007–2019) showed that the seagrass distribution in VFB has declined 46.5–87.2 ha (or 12.2–16.8%) per decade. The losses of seagrass beds and the development of local infrastructures/aquaculture activities as well as the occurrence of natural disasters appeared to be related, and these cause and effect relationships need further research. The impact of these activities and the effects of natural disturbances as causes of the degradation and decline of seagrass beds are currently poorly understood. Our study demonstrated the usefulness of remote sensing data for monitoring seagrass beds at VPB and determining possible causes for seagrass population declines. Our future studies will extend to other important seagrass beds in other regions of Vietnam.

Supplementary Material

Table S1. Coordination of selected different substratum in different years at Tuan Le, Xuan Tu and My Giang. 2A-2D, 3A-3C and 4A-4C are kinds of substratum presented in Figure 2, 3 and 4, respectively.

Table S2. Confusion matrix of the comparison between Landsat image classification result and ground reference data (validation data set) at TL in 2019.

The Supplementary Material is available at https://www.alr-journal.org/10.1051/alr/2020005/olm.

Acknowledgements. We are deeply indebted to all staff of Department of Applied Physics, Nha Trang Institute of Technology Research and Application (NITRA), Vietnam, and the Department of Marine Botany, Center for Oceanographic Data, GIS and Remote Sensing, Institute of Oceanography (IO), Vietnam for logistical support, critically reading the manuscript and generously providing many valuable suggestions. We thank two anonymous reviewers for many constructive suggestions to improve the manuscript. This work was supported by the "National Program on Space Science and Technology" (VT-UD.01/17-20).

References

Anton A, Cebrian J, Duarte MC, Heck LK, Goff J. 2009. Low impact of hurricane Katrina on seagrass community structure and functioning in the northern Gulf of Mexico. *Bull Mar Sci* 85: 45–59.

Barillé L, Robin M, Harin N, Bargain A, Launeau P. 2010. Increase in seagrass distribution at Bourgneuf Bay (France) detected by spatial remote sensing. *Aquat Bot* 92: 185–194.

Bourque AS., Kenworthy WJ, Fourqurean JW. 2015, Impacts of physical disturbance on ecosystem structure in subtropical seagrass meadows. *Mar Ecol Prog Ser* 540: 27–41.

Chen CF, Lau VK, Chang NB, Son NT, Tong PHS, Chiang SH. 2016. Multi-temporal change detection of seagrass beds using integrated Landsat TM/ETM+/OLI imageries in Cam Ranh Bay, Vietnam. *Ecol Inf* 35: 43–54.

Cohen J. 1960. A coefficient of agreement for nominal scales. *Educ Psychol Meas* 20: 37–46.

Colin PL. 2018. *Thalassodendron ciliatum* (Cymodoceaceae) in Palau: Occurrence, typhoon impacts and changes over time. *Bot Mar* 61: 537–546.

Congalton RG. 1991. A review of assessing the accuracy of classifications of remotely sensed data. *Remot Sens Environ* 37: 35–46.

De Vos CHR, Schat H, De Waal MAM, Vooijs R, Ernst WHO. 1991. Increased resistance to copper-induced damage of the root cell

plasmalemma in copper tolerant *Silene cucubalus*. *Physiol Plant* 82: 523–528.

Duarte CM, Borum J, Short FT, Walker DI. 2008. Seagrass ecosystems: their global status and prospects. In: Polunin NVC (Ed.) Aquatic Ecosystems: Trends and Global Prospects. Cambridge: Cambridge University Press, pp. 281–294.

Duffy JP, Pratt L, Anderson K, Land PE, Shutler JD. 2018. Spatial assessment of intertidal seagrass meadows using optical imaging systems and a lightweight drone. *Estuar Coast Shelf Sci* 200: 169–180.

Dung TTT, Cappuyns V, Swennen R, Vassilieva E, Phung NK. 2014. Leachability of arsenic and heavy metals from blasted copper slag and contamination of marine sediment and soil in Ninh Hoa district, south central of Vietnam. *Appl Geochem* 44: 80–92.

Fortes MD. 2012. Historical review of seagrass research in the Philippines. *Coast Mar Sci* 35: 178–181.

Fortes MD, Ooi JLS, Tan YM, Prathep A, Bujang JS, Yaakub SM. 2018. Seagrass in Southeast Asia: A review of status and knowledge gaps, and a road map for conservation. *Bot Mar* 63: 269–288.

Fourqurean WJ, Rutten ML. 2004. The impact of hurricane Georges on soft-bottom, back reef communities: Site- and species-specific effects in south Florida seagrass beds. *Bull Mar Sci* 75: 239–257.

Fraser MW, Kendrick GA. 2017. Belowground stressors and long-term seagrass declines in a historically degraded seagrass ecosystem after improved water quality. *Sci Rep* 7: 14469.

Gacia E, Duarte CM, Marbà N, Terrados J, Kennedy H, Fortes MD, Tri NH. 2003. Sediment deposition and production in SE-Asia seagrass meadows. *Estuar Coast Shelf Sci* 56: 909–919.

Govers LL, Lamers LPM, Bouma TJ, de Brouwer JHF, van Katwijk MM. 2014. Eutrophication threatens Caribbean seagrasses – an example from Curacao and Bonaire. *Mar Pollut Bull* 89: 481–486.

Hedley JD, Harborne AR, Mumby PJ. 2005. Simple and robust removal of sun glint for mapping shallow-water benthos. *Int J Remote Sens* 26: 2107–2112.

Herbeck LS, Sollich M, Unger D, Holmer M, Jennerjahn TC. 2014. Impact of pond aquaculture effluents on seagrass performance in NE Hainan, tropical China. *Mar Pollut Bull* 85: 190–203.

Herbeck LS, Unger D, Wu Y, Jennerjahn TC. 2013. Effluent, nutrient and organic matter export from shrimp and fish ponds causing eutrophication in coastal and back-reef waters of NE Hainan, tropical China. *Cont Shelf Res* 57: 92–104.

Hiraoka KY, Omichi Y, Okada M. 2016. Recovery of natural *Zostera* bed after typhoon attacks and autonomous restoration of *Zostera* bed by backfilling old navigation channel at the mouth of Imazu river in Hiroshima Bay. *J Jpn Soc Water Environ* 39: 97–102 (in Japanese with English abstract)

Honda K, Nakamura Y, Nakaoka M, Uy WH, Fortes MD. 2013. Habitat use by fishes in coral reefs, seagrass beds and mangrove habitats in the Philippines. *PloS ONE* 8: e65735.

Hossain MS, Bujang JS, Zakaria MH, Hashim M. 2015. The application of remote sensing to seagrass ecosystems: An overview and future research prospects. *Int J Remote Sens* 36: 61–114.

Jaxion-Harm J, Saunders J, Speight MR. 2012. Distribution of fish in seagrass, mangroves and coral reefs: Life-stage dependent habitat use in Honduras. *Rev Biol Trop* 60: 683–698.

Kim K, Choi JK, Ryu JH, Jeong HJ, Lee K, Park MG, Kim KY. 2015. Observation of typhoon-induced seagrass die-off using remote sensing. *Estuar Coast Shelf Sci* 154: 111–121.

Kirkman H, Kirkman JA. 2002. The management of seagrasses in Southeast Asia. *Bull Mar Sci* 71: 1379–1390.

Le AT, Nguyen DM. 2004. Present status of lobster cage culture in Vietnam. In: Williams KC (Ed.) Spiny lobster ecology and exploitation in the South China Sea region. ACIAR Proceedings, Vol 120. Australian Centre for International Agriculture Research, Canberra, pp. 21–25.

Lemmens J, Clapin G, Lavery P, Cary J. 1996. Filtering capacity of seagrass meadows and other habitats of Cockburn Sound, Western Australia. *Mar Ecol Progr Ser* 143: 187–200.

Lyzenga DR. 1978. Passive remote sensing techniques for mapping water depth and bottom features. *Appl Optics* 17: 379–383.

McCloskey RM, Unsworth RKF. 2015. Decreasing seagrass density negatively influences associated fauna. *PeerJ* 3: e1053.

McKenna S, Jarvis J, Sankey T, Reason C, Coles R, Rasheed M. 2015. Declines of seagrasses in a tropical harbour, North Queensland, Australia, are not the result of a single event. *J Biosci* 40: 389–398.

Montefalcone M, Albertelli G, Nike Bianchi C, Mariani M, Morri C. 2006. A new synthetic index and a protocol for monitoring the status of *Posidonia oceanica* meadows: A case study at Sanremo (Ligurian Sea, NW Mediterranean). *Aquat Conserv* 16: 29–42.

Nadiarti, Riani E, Djuwita I, Budiharsono S, Purbayanto A, Asmus H. 2012. Challenging for the seagrass management in Indonesia. *J Coast Dev* 15: 234–242.

Neckles HA, Kopp BS, Peterson BJ, Pooler PS. 2012. Integrating scales of seagrass monitoring to meet conservation needs. *Estuar Coasts* 35: 23–46.

Neckles HA, Short FT, Barker S, Kopp BS. 2005. Disturbance of eelgrass *Zostera marina* by commercial mussel *Mytilus edulis* harvesting in Maine: Dragging impacts and habitat recovery. *Mar Ecol Prog Ser* 285: 57–73.

Nguyen XH, Nguyen NNT. 2014. Current status and trends of mangroves and seagrass in Van Phong Bay, Khanh Hoa province. *Coll Mar Works* 21: 201–211 (in Vietnamese with English abstract)

Nguyen XV, Pham TL, Nguyen NNT, Nguyen TH. 2010. Final report: Monitoring of seagrass beds, mangrove forests in Khanh Hoa province. Department of Natural Resource and Environment of Khanh Hoa province., 45 pp (in Vietnamese)

Nguyen XV, Tran MH, Le TD, Papenbrock J. 2017a. An assessment of heavy metal contamination on the surface sediment of seagrass beds at the Khanh Hoa Coast, Vietnam. *Bull Environ Contam Toxicol* 99: 728–734.

Nguyen XV, Tran MH, Papenbrock J. 2017b. Different organs of *Enhalus acoroides* (Hydrocharitaceae) can serve as specific bioindicators for sediment contaminated with different heavy metals. *S Afr J Bot* 113: 389–395.

Nordlund LM, Unsworth RKF, Gullström M, Cullen-Unsworth LC. 2018. Global significance of seagrass fishery activity. *Fish Fisheries* 19: 399–412.

Orth RJ, Carruthers TJB, Dennison WC, Duarte CM, Fourqurean JW, Heck KL, Hughes AR, Kendrick GA, Kenworthy WJ, Olyarnik S, Short FT, Waycott M, Williams SL. 2006. A global crisis for seagrass ecosystems. *BioScience* 56: 987–996.

Papenbrock J. 2012. Highlights in seagrasses' phylogeny, physiology, and metabolism: What makes them special? *Int Scholar Res Netw Bot* 2012: 15.

Pham HT, Nguyen HD, Nguyen XH, Nguyen TL. 2006, Study on the variation of seagrass population in coastal waters of Khanh Hoa Province, Vietnam. *Coast Mar Sci* 30: 167–173.

Poiner IR, Walker DI, Coles RG. 1989. Regional studies: Seagrasses of tropical Australia. In: Larkum AWD, McComb AJ, Shepherd SA (Eds.). Biology of Seagrasses: Aquatic Plant Studies 2. Amsterdam: Elsevier, pp. 279–303.

Preen AR, Lee Long WJ, Coles RG. 1995. Flood and cyclone related loss, and partial recovery, of more than 1000 km^2 of seagrass in Hervey Bay, Queensland, Australia. *Aquat Bot* 52: 3–17.

Rattanachot E, Stankovic M, Aongsara S, Prathep A. 2018. Ten years of conservation efforts enhance seagrass cover and carbon storage in Thailand. *Bot Mar* 61: 441–452.

Royo CL, Gérard P, Pergent-Martini C, Casazza G. 2010. Seagrass (*Posidonia oceanica*) monitoring in western Mediterranean: Implications for management and conservation. *Envir Monit Assess* 171: 365–380.

Ruiz JM, Pérez M, Romero J. 2001. Effects of fish farm loadings on seagrass (*Posidonia oceanica*) distribution, growth and photosynthesis. *Mar Pollut Bull* 42: 749–760.

Sabol MB, Melton RE, Chamberlain R, Doering P, Haunert K. 2002. Evaluation of a digital echo sounder system for detection of submersed aquatic vegetation. *Estuaries* 25: 133–141.

Sagawa T, Boisnier E, Komatsu T, Mustapha KB, Hattour A, Kosaka N, Miyazaki S. 2010. Using bottom surface reflectance to map coastal marine areas: A new application method for Lyzenga's model. *Int J Remote Sens* 31: 3051–3064.

Schultz ST. 2008. Seagrass monitoring by underwater videography: Disturbance regimes, sampling design, and statistical power. *Aquat Bot* 88: 228–238.

Scott AL, York PH, Duncan C, Macreadie PI, Connolly RM, Ellis MT, Jarvis JC, Jinks KI, Marsh H, Rasheed MA. 2018. The role of herbivory in structuring tropical seagrass ecosystem service delivery. *Front Plant Sci* 9: 127.

Short FT, Koch EW, Creed JC, Magalhães KM, Fernandez E, Gaeckle JL. 2006. SeagrassNet monitoring across the Americas: case studies of seagrass decline. *Mar Ecol* 27: 277–289.

Steward JS, Virnstein RW, Lasi MA, Morris LJ, Miller JD, Hall LM, Tweedale WA. 2006. The impacts of the 2004 hurricanes on hydrology, water quality, and seagrass in the central Indian River Lagoon, Florida. *Estuar Coast* 29: 954–965.

Tu DV, de Montaudouin X, Blanchet H, Lavesque N. 2012. Seagrass burial by dredged sediments: benthic community alteration, secondary production loss, biotic index reaction and recovery possibility. *Mar Pollut Bull* 64: 2340–2350.

Uhrin AV, Fonseca SM. 2005, Effect of Caribbean spiny lobster traps on seagrass beds of the Florida Keys National Marine Sanctuary: Damage sssessment and evaluation of recovery. *Am Fish Soc Symp* 41: 579–588.

Uhrin AV, Turner MG. 2018. Physical drivers of seagrass spatial configuration: the role of thresholds. *J Landsc Ecol* 33: 2253–2272.

Vanhellemont Q. 2019. Adaptation of the dark spectrum fitting atmospheric correction for aquatic applications of the Landsat and Sentinel-2 archives. *Remote Sens Environ* 225: 175–192.

Vanhellemont Q, Ruddick K. 2018. Atmospheric correction of metre-scale optical satellite data for inland and coastal water applications. *Remote Sens Environ* 216: 586–597.

Waycott M, Duarte CM, Carruthers TJ, Orth RJ, Dennison WC, Olyarnik S, Calladine A, Fourqurean JW, Heck KL, Jr., Hughes AR, Kendrick GA, Kenworthy WJ, Short FT, Williams SL. 2009. Accelerating loss of seagrasses across the globe threatens coastal ecosystems. *Proc Nat Acad Sci USA* 106: 12377–12381.

Yang D, Huang D. 2011. Impacts of typhoons Tianying and Dawei on seagrass distribution in Xincun Bay, Hainan province, China. *Acta Oceanol Sin* 30: 32–39.

Yang D, Yang C. 2009. Detection of seagrass distribution changes from 1991 to 2006 in Xincun Bay, Hainan, with satellite remote sensing. *Sensors* 9: 830–844.

Yang D, Yang C. 2014. Effects of typhoon on seagrass distribution. In: Tang DL, Sui G (Eds.), Typhoon Impact and Crisis Management. Berlin: Springer-Verlag, pp. 253–266.

Cite this article as: Vo T-T, Lau K, Liao LM, Nguyen X-V. 2020. Satellite image analysis reveals changes in seagrass beds at Van Phong Bay, Vietnam during the last 30 years. *Aquat. Living Resour.* 33: 4